scribed by Lykke *et al.* (23). Owing to the lack of an additional sample, further investigation into the origin of the fragments was precluded. Thus, their origin is indeterminate at this time.

The vapor environment in which fullerenes can form and then persist is of interest. The first step in fullerene formation involves vaporization of carbon into atoms, dimers, or both (24, 25). In our case, the fullerenes that were contained within the fulgurite formed in the presence of many other gases. These include all atmospheric gases in the lightning channel as well as materials vaporized on the ground by the strike. The techniques used to synthesize fullerenes provide evidence that fullerenes can form while in the presence of other gases. For example, in the combustion process, fullerenes form in the presence of hydrogen and oxygen (4, 5). In the laser ablation of polymers as well as of coals, fullerenes form in vapors containing nitrogen, sulfur, hydrogen, and oxygen (26–28). Bombardment of a polymer containing fluorine and hydrogen by a $^{127}I^{14+}$-MeV ion beam also produced fullerenes (6). Essene and Fisher (10) described highly reduced phases in a fulgurite, clearly indicating that the immediate, local region can differ greatly from the surrounding ambient environment. In this case also, the extreme effects of lightning are evident and were apparently conducive to fullerene formation.

Finally, Chibante *et al.* (29) indicate that fullerenes have finite lifetimes in the ambient air. The Sheep Mountain sample was collected in about 1980 (by C. F. Lewis) and appeared so fresh and free of breakage and sharp edges that it probably had not experienced the weathering associated with seasonal cycles.

The peculiar association of fullerenes with a fulgurite strongly suggests to us that the lightning was the causative agent for both. The only other fullerenes reported from the terrestrial environment occur in shungite (7), a coal-like rock found in Karelia, Russia. An obvious question is whether the formative agent for the shungite material was lightning. Unfortunately, we did not observe the shungite sample in the field, and so we cannot be certain that it is unrelated to a lightning strike. However, the occurrence of fullerenes in thin veinlets and the absence of evidence of localized melting, such as is typical of fulgurites, argue against an origin related to lightning. We thus tentatively conclude that the two samples have distinct geological histories and that their fullerenes are unrelated in origin.

REFERENCES AND NOTES

1. H. W. Kroto *et al.*, *Nature* **318**, 162 (1985).
2. W. Krätschmer *et al.*, *ibid.* **347**, 354 (1990).
3. W. Krätschmer, K. Fostiropoulos, D. R. Huffman, *Chem. Phys. Lett.* **170**, 167 (1990).
4. J. T. McKinnon, W. L. Bell, R. M. Barkley, *Combust. Flame* **88**, 102 (1992).
5. J. B. Howard *et al.*, *Nature* **352**, 139 (1991).
6. G. Brinkmalm *et al.*, *Chem. Phys. Lett.* **191**, 345 (1992).
7. P. R. Buseck, S. J. Tsipursky, R. Hettich, *Science* **257**, 215 (1992).
8. R. C. Jones, *J. Geophys. Res.* **73**, 809 (1968).
9. G. Frenzel and V. Stähle, *Chem. Erde* **41**, 111 (1982).
10. E. J. Essene and D. C. Fisher, *Science* **234**, 189 (1986).
11. R. Clocchiatti, *Eur. J. Mineral.* **2**, 479 (1990).
12. D. H. Parker *et al.*, *J. Am. Chem. Soc.* **113**, 7499 (1991).
13. D. Askaren, personal communication.
14. P. W. Lipman, *Evolution of the Platoro Caldera Complex and Related Volcanic Rocks, Southeastern San Juan Mountains, Colorado* [*U.S. Geol. Surv. Prof. Pap. 852* (1975)].
15. M. A. Uman and E. P. Krider, *Science* **246**, 457 (1989).
16. B. F. J. Schonland, *Proc. R. Soc. London Ser. A* **164**, 132 (1938).
17. M. A. Uman, *The Lightning Discharge* (International Geophysics Series, vol. 39, Academic Press, Orlando, FL, 1987), chaps. 1, 7, 15.
18. M. Brook, N. Kitagawa, E. J. Workman, *J. Geophys. Res.* **67**, 649 (1962).
19. R. E. Orville, *J. Atmos. Sci.* **25**, 827 (1968).
20. R. D. Hill, *J. Geophys. Res.* **76**, 637 (1971).
21. H. Ajie *et al.*, *J. Phys. Chem.* **94**, 8630 (1990).
22. C. Yeretzian *et al.*, *Nature* **359**, 44 (1992).
23. K. R. Lykke *et al.*, *Mater. Res. Soc. Symp. Proc.* **206**, 679 (1991).
24. J. R. Heath, in *Fullerenes: Synthesis, Properties, and Chemistry of Large Carbon Clusters*, G. S. Hammond and V. J. Kuck, Eds. (American Chemical Society Symposium Series 481, Washington, DC, 1992), chap. 1.
25. T. W. Ebbesen, J. Tabuchi, K. Tanigaki, *Chem. Phys. Lett.* **191**, 336 (1992).
26. W. R. Creasy and J. T. Brenna, *Chem. Phys.* **126**, 453 (1988).
27. ______, *J. Chem. Phys.* **92**, 2269 (1990).
28. P. F. Greenwood, M. G. Strachan, G. D. Willett, M. A. Wilson, *Org. Mass Spectrom.* **25**, 353 (1990).
29. L. P. F. Chibante, C. Pan, M. L Pierson, R. E. Haufler, D. Heymann, *Carbon*, in press.

30. We thank J. Holloway and S. Williams, who looked at the thin section of the sample, and J. Clark, who provided electron microprobe analyses. Helpful discussions about lightning were held with P. Krider and about fulgurites with R. Hervig. W. Lehman assisted with the mass spectrometry. D. Askaren informed us about the Sheep Mountain stratigraphy. We thank E. Essene, D. New, V. Barnes, and S. Sorensen for providing fulgurites, and Chau-Wen Chou and Cong-Wen Lou for computer assistance. This study was supported by National Science Foundation (NSF) grant EAR-8708529 to P.R.B. The electron microprobe was obtained through NSF grant EAR-8408168. The TOF system was built with funds from NSF grant CHE-900639 and Department of Energy grant DE-FG02-91ER61127 granted to P.W.

2 November 1992; accepted 31 December 1992

Buckytubes and Derivatives: Their Growth and Implications for Buckyball Formation

V. P. Dravid, X. Lin, Y. Wang, X. K. Wang, A. Yee, J. B. Ketterson, R. P. H. Chang

Transmission electron microscopy (TEM) observations of graphite tubules (buckytubes) and their derivatives have revealed not only the previously reported buckytube geometries but also additional shapes of the buckytube derivatives. Detailed cross-sectional TEM images reveal the cylindrical cross section of buckytubes and the growth pattern of buckytubes as well as their derivatives. These observations of frozen growth stages of buckytubes and derivatives suggest a helical growth mechanism analogous to that of crystal growth via screw dislocations. The helicacy of buckytubes is analyzed by electron diffraction whereas the anisotropy of electronic structure is revealed by momentum transfer resolved electron energy loss spectrometry. Based on the TEM observations, it is proposed that buckytubes act as precursors to closed-shell fullerene (buckyball) formation and the possible steps in buckyball formation are outlined. In arc evaporation experiments in which residue rods (containing various amounts of buckytubes) were used as the starting anode for fullerene production, the amount of buckytubes in the rod was correlated with fullerene yield.

The synthesis, characterization, and properties of various all-carbon molecules, the fullerene family (buckyballs), have been on the research forefront since the large-scale production scheme developed by Krätschmer *et al.* (1). Recently, Iijima and co-workers (2–4) reported TEM observations of hollow graphitic tubules of nanometer scale (buckytubes). In particular, the large-scale buckytube synthesis method of Ebbesen and Ajayan (5) has stirred considerable interest similar to that after the Krätschmer *et al.* (1) discovery of large-scale buckyball synthesis.

We have synthesized gram-scale quantities of buckytubes and their derivatives based on an arc method similar to that of Ebbesen and Ajayan (5, 6). Most of the TEM observations were made by scraping the transition region between the "black ring" material and the outer shell and then dispersing the powder on a holey carbon TEM grid. Additional experiments were

Materials Research Center, Northwestern University, Evanston, IL 60208.

conducted by preparing cross sections of the rod such that the interface between the black ring and the outer shell of the rod was electron-transparent and roughly parallel to the electron beam. High-resolution TEM images revealed all of the previously reported forms of buckytubes, such as tubes with a varying number of shells, tubes with capped ends, and the intermediate structures proposed (3) to consist of pentagons, heptagons, and elements with negative curvatures.

At higher magnification (see Fig. 1A), we observed that the rounded particulates in the transition region between the "black ring" and the outer shell of the residue rod are a collection of completely closed graphitic sheets with a helical pattern of inner shells. Although these features appear to have toroidal shape in projection, tilting experiments indicate that they are completely closed in three dimensions. Such unusual particulates are intrinsically present in transition regions of the residue rod and are not a consequence of electron beam effect, as demonstrated by Ugarte (7). These particulates may best be described as faceted buckyfootballs [or onions (7)] and offer interesting evidence for their growth. If we follow the individual inner shell graphitic sheets around, we observe that the termination is incomplete, that is, one extra graphitic sheet is associated with one portion of the inner shell compared with its opposite side. Other larger buckyfootballs contain smaller inner footballs that seem to grow inside the larger one (Fig. 1B). The inner footballs clearly display extra unterminated graphitic sheets indicative of helical growth. These observations strongly suggest that Fig. 1, A and B, represent buckyfootballs that form through a helical growth of the sheets analogous to that of single-crystal growth through a screw dislocation mechanism (2).

Conceivably, one can invoke a similar helical growth mechanism for the long or straight buckytubes, as suggested previously (2). Cross-sectional TEM images of buckytubes (Fig. 1, C and D) display the circular cross section of buckytubes and their growth pattern. Elastic strain contrast due to linear defects [presumably disclination-type defects (2)] is also apparent in these images. One extra (unterminated) sheet can be observed for each of the buckytubes in Fig. 1C, whereas three or more graphitic shells are seen to wrap around a thicker buckytube (arrow, Fig. 1D). Thus, it appears that helical growth is a viable mechanism for buckytube growth as well. The growth process, however, appears to take place from inside (as in Fig. 1, A and B) as well as outside (as in Fig. 1D). The details of the time-resolved kinetics of growth of buckytube derivatives may be quite complicated, as can be appreciated from Fig. 1E, which shows a small buckytube completely encapsulated in a larger one. The inner buckytube in Fig. 1E does not have any direct access to carbon source. An understanding of growth processes for such morphologies requires more observations on the intermediate stages of growth. Nonetheless, the growth of all other types of buckytubes and footballs where there are no terminations or caps may still occur by the helical

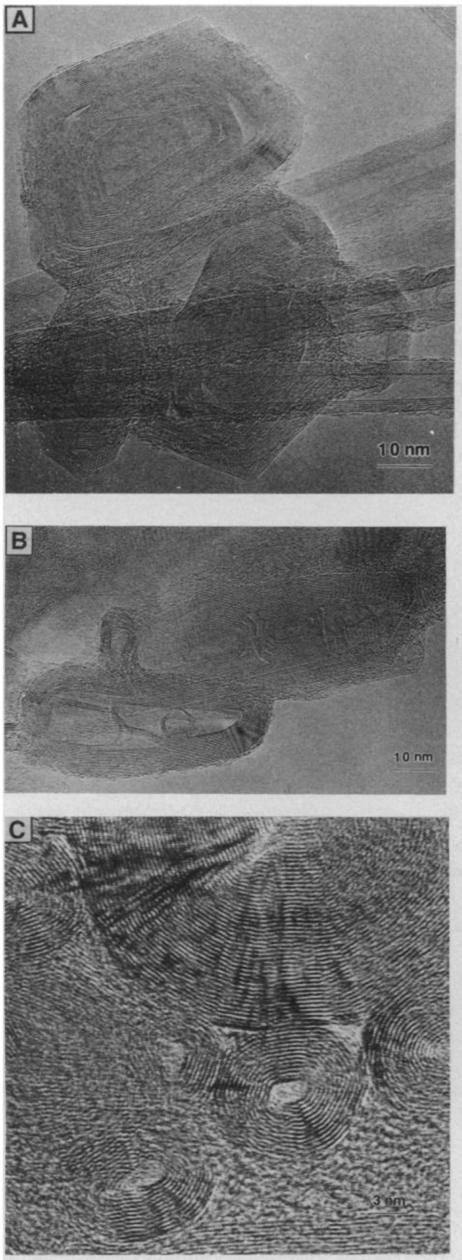

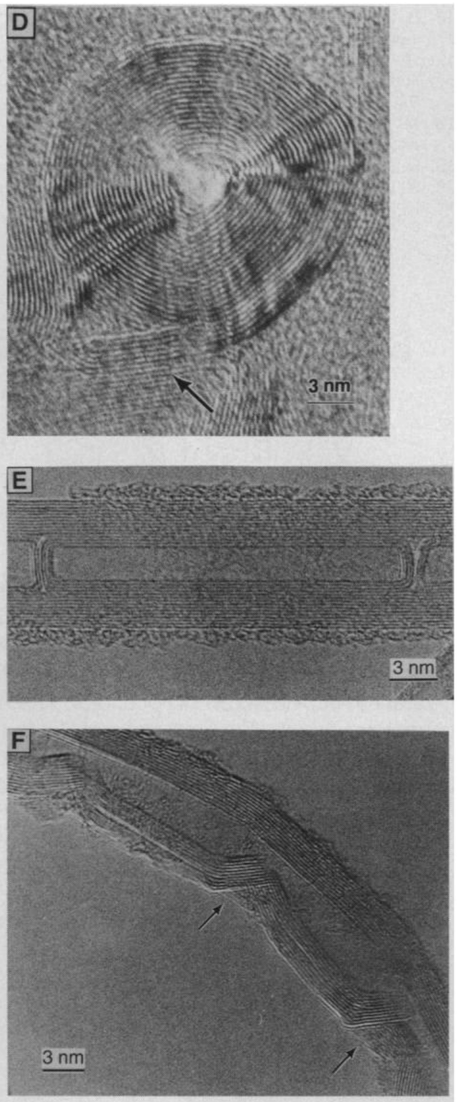

Fig. 1. (**A**) A TEM image of buckyfootballs. Inner graphitic sheets are not closed completely. (**B**) Three small buckyfootballs appear to grow inside a large buckyfootball. (**C** and **D**) Cross-sectional TEM images of buckytubes. (C) A large buckytube and smaller ones are seen end-on. The smaller buckytubes have extra unterminated sheets. (D) Frozen growth of a buckytube seen end-on. As many as four graphite sheets are seen to wrap around the buckytube. (**E**) A buckytube of two layers appears to be completely trapped in a larger buckytube. (**F**) A high-resolution TEM image of a broken and bent buckytube.

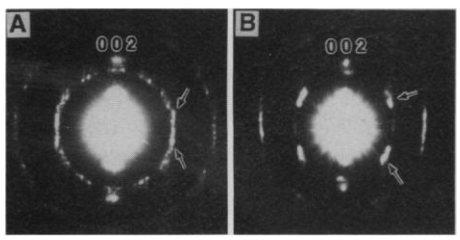

Fig. 2. Two representative electron diffraction patterns from two buckytubes, (**A**) a 13-shell buckytube and (**B**) a 5-shell buckytube. The helicity of the tubes is reflected in the rotation of {100}- and {110}-type spots (arrows) with respect to the {002} reflections. Calculations indicate that the 13-shell buckytube has two sets of helicacy, whereas the 5-shell tube has only one.

growth mechanism, either from inside (Fig. 1, A and B) or from outside (Fig. 1, C and D).

The helicacy of buckytubes is an interesting phenomenon. It has been suggested (*2, 8–11*) that the growth pattern as well as many properties of buckytubes are intimately related to their helicacy. Iijima (*2*) has indicated that electron diffraction patterns reveal the helicacy of the tubes in the form of diffraction spot rotations and streaks in the diffraction patterns. We have carried out a systematic study of electron diffraction of buckytubes as a function of number of shells. We observe that a large number of one- or two-shell buckytubes have a unit translation (in closure) associated with them. Representative electron diffraction patterns from two different buckytubes, one with 13 shells and the other with 5 shells, are shown in Fig. 2, A and B, respectively. The angular relation between the {002} spot and the other spots is a measure of the helicacy, whereas the streaking of the diffraction maxima along the *c*-axis is due to the shape (and size) effect as well as to the curved nature of the graphite sheets. Diffraction simulations based on dynamical theories of electron diffraction confirm that the 13-shell buckytubes have two sets of helicacy whereas the 5-shell buckytube has only one set (*12*).

We have also compared the electron energy loss spectra (EELS) of buckytubes to those of conventional graphite. Subtle but significant deviations in spectral features and their energy are noted. The low loss transitions for buckytubes are always shifted to lower energies than those of graphite, indicating a loss of valence electrons and a change in band gap, which are most likely related to the curved nature of the graphitic sheets (Fig. 3A). The core loss spectra of buckytubes are compared with those of graphite under similar momentum transfer conditions. Two geometries have been used to highlight the differences, one in which the electron beam is parallel to the tube axis (case I, Fig. 3B) and the other in which the buckytube axis is normal to the electron beam (case II, Fig. 3C). In case I, although the sheets are curved, the common *c*-axis of all of the sheets is radially perpendicular to the electron beam. The resultant core-loss EELS spectrum is virtually identical to that of graphite under similar geometry. However, case II spectra are substantially different. In case II geometry, although the tube axis is normal to the electron beam, the {002} planes are constantly changing angle with respect to the electron beam, which leads to a greater σ^* contribution to the EELS spectra of buckytubes. As the number of shells in the buckytube increases, both the low loss and the core loss spectra assume the typical graphite transitions, both in energy and spectral shapes. The strong anisotropy of the electronic structure of buckytubes as deduced from the EELS spectra should reflect in the electronic and magnetic properties of these strongly anisotropic structures, as is also suggested by theoretical calculations (*8–11*).

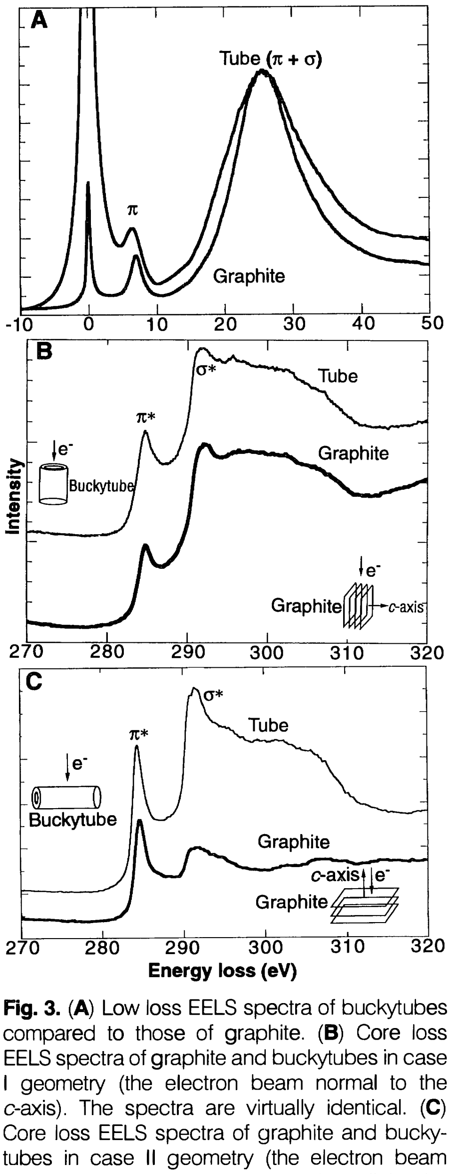

Fig. 3. (**A**) Low loss EELS spectra of buckytubes compared to those of graphite. (**B**) Core loss EELS spectra of graphite and buckytubes in case I geometry (the electron beam normal to the *c*-axis). The spectra are virtually identical. (**C**) Core loss EELS spectra of graphite and buckytubes in case II geometry (the electron beam parallel to the *c*-axis of graphite and parallel to the tube axis). The additional σ^* contribution to the buckytube spectrum is attributed to the curved nature of the buckytube graphitic sheets.

The existence of buckytubes in the residue rod of the cathode electrode of the arc has led us to speculate that if the pristine graphite rods can generate soot that contains C_{60}, then buckytubes ought to be a much more efficient precursor for buckyball (C_{60}) and higher fullerene formation. Buckytubes in the close vicinity of the arc might become fragmented in a manner that would result in short length (capped or uncapped) buckytubes. These short segments of buckytubes (linear dimension roughly equal to their diameter) may escape the graphite rod and close in a variety of ways. Those buckytube fragments, which have the critical number of carbon atoms as well as the number of hexagons and pentagons, may eventually form closed shell fullerenes of 60 or more carbon atoms. Those that do not satisfy the number of carbon atoms or hexagon-pentagon criteria or both may dissociate rapidly to form other carbon residues that form during fullerene synthesis.

One of the other unusual geometries that we have observed is shown in Fig. 1F. The bending of the tubes sometimes fracture the "elbows" of the buckytubes (arrows) where the fractured elbows appear to have been reconstructed. The elbow regions may be frozen stages of buckyball formation. If the broken buckytubes escape and reconstruct in the carbon mist, they may lead to closed shell fullerene formation. We have seen an appreciable number of broken buckytubes (buckyboomerangs) in the region of the residue rod that is at the tip of the arc. Such observations support the conjecture that the broken buckytubes may be the precursors to buckyball formation. In this view, Fig. 1F perhaps represents a frozen stage of buckytubes prior to total fragmentation and escape as buckyballs or residue or both.

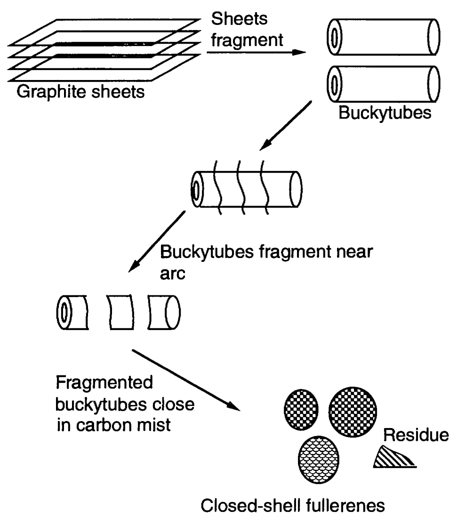

Fig. 4. Schematic illustration of the formation of buckyballs via buckytubes.

To substantiate our hypothesis that buckytubes may be a more efficient precursor for buckyball formation, we performed the following comparison experiments. Separate batches of soot were generated with two different starting anode rods, a standard graphite rod and a redeposited residue rod with a substantial amount of buckytubes present. The fraction C_{60} was separated from the soot using a standard recirculating Wudl system (*13*). For the graphite rod, the soot contained ~10.1% C_{60}. For residue rods with buckytubes, the percentage yield of C_{60} was in the range of 20 to 60%, depending on the percentage of buckytubes present in the rod. The relative amount of higher fullerene (greater than C_{70}) has also increased from our soot separation. The fullerene yield correlated well with the number density of buckytubes in the residue rod, that is, the larger the number of buckytubes, the more the yield of fullerenes.

The possible steps in closed shell fullerene formation are outlined in Fig. 4. The first step includes tearing of graphite sheets in the vicinity of the arc. The folding of the graphite sheets would lead to buckytube formation. Recent theoretical work (*11, 14*) suggests that a tubular morphology is favored over a flat sheet under certain geometrical conditions. The number of sheets and their length determine the diameter of the buckytubes and their linear length. These buckytubes may become fragmented at the arc tip, which would lead to further closing of the open end or ends of the fragmented buckytubes in the carbon mist of the arc. Statistical consideration may dictate the critical number of carbon atoms and their configuration (that is, number of hexagons and pentagons). Those that obey the critical conditions may close their shells on separation or, alternatively, as they pass through the stream of atomic carbon in the arc, escaping as fullerenes in either case. Those that do not satisfy the number and geometrical requirements may rapidly dissociate to form lower fullerenes or carbon residue or both. The higher yield of C_{60} fullerenes may be associated with the growth kinetics of buckytubes where the innermost shell is perhaps all alone in the vicinity of the arc. The fragmentation of the inner shells is likely to produce more C_{60} than higher fullerenes. The closed shell fullerenes, thus formed, may either dissociate to lower fullerenes or residue or both if the geometry and number criteria are not satisfied or may land as fullerenes (C_{60}, C_{70}, and so forth).

REFERENCES AND NOTES

1. W. Krätschmer, L. D. Lamb, K. Fostiropoulos, D. R. Huffman, *Nature* **347**, 354 (1990).
2. S. Iijima, *ibid.* **354**, 56 (1991).
3. ———, T. Ichihashi, Y. Ando, *ibid.* **356**, 776 (1992).
4. P. M. Ajayan and S. Iijima, *ibid.* **358**, 23 (1992).
5. T. W. Ebbesen and P. M. Ajayan, *ibid.*, p. 220.
6. The arc was formed between a 1-inch and a 1/2-inch diameter (2.5 to 1.25 cm) graphite rods under 100 torr of helium at 180 to 200 A and 20 to 30 V. In the arc process, the 1-inch graphite rod (cathode) is generally unaffected but the 1/2-inch rod (anode) is consumed, while a roughly 1/2-inch rod (residue) builds up on the original unconsumed 1-inch graphite rod. The cross section of the resulting buildup rod consists of a gray core, followed by a black ring and another gray shell. The black ring in the middle consists of large number of buckytubes, many millimeters in length with a range of diameters. The transition region between the "black ring" and the outer shell consists of closed-shell particulate derivatives.
7. D. Ugarte, *Nature* **359**, 707 (1992).
8. M. S. Dresselhaus, G. Dresselhaus, R. Sato, *Phys. Rev. B* **45**, 6234 (1992).
9. R. Sato *et al.*, *ibid.* **46**, 1804 (1992).
10. ———, *Appl. Phys. Lett.* **60**, 2204 (1992).
11. N. Hamada, S. Sawada, A. Oshiyama, *Phys. Rev. Lett.* **68**, 1579 (1992).
12. V. P. Dravid *et al.*, unpublished results.
13. K. Kahemani, M. Prato, F. Wudl, *J. Org. Chem.* **57**, 3254 (1992).
14. S. Sawada and N. Hamada, *Solid State Commun.*, in press.

13 October 1992; accepted 26 January 1993

Betacellulin: A Mitogen from Pancreatic β Cell Tumors

Y. Shing, G. Christofori, D. Hanahan, Y. Ono, R. Sasada, K. Igarashi, J. Folkman*

Betacellulin, a member of the epidermal growth factor family, has been identified in the conditioned medium of cell lines derived from mouse pancreatic β cell tumors. Betacellulin is a 32-kilodalton glycoprotein that appears to be processed from a larger transmembrane precursor by proteolytic cleavage. The carboxyl-terminal domain of betacellulin has 50 percent sequence similarity with that of rat transforming growth factor α. Betacellulin is a potent mitogen for retinal pigment epithelial cells and vascular smooth muscle cells.

It is increasingly evident that carcinogenesis involves a series of genetic and epigenetic changes that together produce a malignant phenotype. Many of these changes are implicated in the aberrant growth control of the tumor cells themselves (*1, 2*) and in the induction of new blood vessel growth (angiogenesis) to the tumors (*3*). Two transgenic mouse models of tumorigenesis have provided evidence that angiogenesis is activated in the late preneoplastic stages, which suggests that the switch to the angiogenic phenotype is a discrete event (*4, 5*). One experimental avenue to study the mechanisms that control both tumor cells and the vascular system is to identify molecules secreted by tumor cells that have mitogenic activity on one or another of the cell types involved in tumor growth. During the course of such experiments, we have identified a growth factor and refer to it as betacellulin.

RIP1-Tag2 mice carry a hybrid oncogene composed of a rat insulin gene regulatory region fused to the coding region of the simian virus 40 (SV40) T antigen gene. These mice develop pancreatic β cell carcinomas (insulinomas) in a multistep process (*6*), and a series of cell lines (called BTC) have been derived from these tumors (*7*). One cell line, BTC-3, is being used for a systematic study of tumor growth and angiogenesis factors. Betacellulin was initially detected as a mitogen for Balb/c 3T3 cells in the conditioned medium of this and another insulinoma-derived cell line, BTC-JC10, and was purified to apparent homogeneity (*8*). Approximately 6 μg of pure betacellulin was isolated from 200 liters of medium. The overall purification was 170,000-fold, with 4% recovery. Purified betacellulin migrated as a single band in SDS–polyacrylamide gel electrophoresis, with an apparent molecular mass of ~32 kD (Fig. 1A). We recovered the mitogenic activity of betacellulin on Balb/c 3T3 cells by extracting the 32-kD protein band from the polyacrylamide gel. Betacellulin stimulated the proliferation of retinal pigment epithelial and vascular smooth muscle cells at a concentration of ~30 pM (1 ng/ml) but did not stimulate the growth of several other cell types, such as endothelial cells and fetal lung fibroblasts (Fig. 1B).

Microsequencing of purified betacellulin protein with a protein sequencer (ABI 477; Applied Biosystems, Foster City, California) provided a partial NH_2-terminal amino acid sequence and three internal sequences. The partial NH_2-terminal sequence A was identified as Asp-Gly-(X)-Thr-(X)-Arg-Thr-Pro-Glu-Thr-Asn-Gly-Ser-Leu-(X)-Gly-Ala-Pro-Gly-Glu-Glu-Arg-Thr (where X represents unidentifiable residues). A computer search through the translated GenBank and NBRE (National Biomedical

Y. Shing, Department of Surgery, Children's Hospital, and Departments of Biological Chemistry and Surgery, Harvard Medical School, Boston, MA 02115.
G. Christofori and D. Hanahan, Department of Biochemistry and Biophysics, Hormone Research Institute, University of California, San Francisco, CA 94143.
Y. Ono, R. Sasada, K. Igarashi, Biology Research Laboratories, Central Research Division, Takeda Chemical Industries, Yodogawa-ku, Osaka 532, Japan.
J. Folkman, Department of Surgery, Children's Hospital, and Departments of Surgery and Anatomy and Cellular Biology, Harvard Medical School, Boston, MA 02115.

*To whom correspondence should be addressed.